Structural Transitions in the Protein L Denatured State Ensemble

Michelle L. Scalley, Sehat Nauli, Sharon T. Gladwin, and David Baker*

Department of Biochemistry, University of Washington, Seattle, Washington 98195

Received May 18, 1999; Revised Manuscript Received August 30, 1999

ABSTRACT: We use a broad array of biophysical methods to probe the extent of structure and time scale of structural transitions in the protein L denatured state ensemble. Measurement of amide proton exchange protection during the first several milliseconds following initiation of refolding in 0.4 M sodium sulfate revealed weak protection in the first β-hairpin and helix. A tryptophan residue was introduced into the first β-hairpin to probe the extent of structure formation in this part of the protein; the intrinsic fluorescence of this tryptophan was found to deviate from that expected given its local sequence context in 2−3 M guanidine, suggesting some partial ordering of this region in the unfolded state ensemble. To further probe this partial ordering, dansyl groups were introduced via cysteine residues at three sites in the protein. It was found that fluorescence energy transfer from the introduced tryptophan to the dansyl groups decreased dramatically upon unfolding. Stopped-flow fluorescence studies showed that the recovery of dansyl fluorescence upon refolding occurred on a submillisecond time scale. To probe the interactions responsible for the residual structure observed in the denatured state ensemble, the conformation of a peptide corresponding to the first β-hairpin and helix of protein L was studied using circular dichroism spectroscopy and compared to that of full-length protein L and previously characterized peptides corresponding to the isolated helix and second β-hairpin.

The kinetics and thermodynamics of the folding of many small proteins have been found to be well described by a two-state folding model (*1*−*8*). Protein L is one such protein; the kinetics of folding measured by stopped-flow circular dichroism (CD),[1] stopped-flow fluorescence, quenched-flow HD exchange, and equilibrium denaturation data from fluorescence experiments are described well by a two-state model (*9*). Also, native-state HD exchange experiments showed no evidence of populated intermediates with free energies between the native and unfolded states under native conditions (*10*).

While the folding of protein L is well described by a two-state model, fluorescence-quenching experiments (*9*) and amide proton exchange protection factors measured from dead-time labeling experiments (*10*) suggested partial ordering of the first β-hairpin and helix in the denatured state under low to intermediate denaturant concentrations. Furthermore, mutagenesis experiments showed that this region is at least partially structured in the folding transition state; mutations within the first β-turn (G15A) significantly slow the folding rate and have high Φ-values (*11*). Here we investigate the ordering of this portion of the protein in the denatured state through (1) dead-time HD exchange under stabilizing conditions, (2) fluorescence experiments on protein L with a tryptophan residue introduced into this region (F20W), (3) measurement of the efficiency of fluorescence energy transfer between F20W and dansyl groups placed throughout the protein, and (4) analysis of peptides of increasing length derived from this region.

METHODS AND MATERIALS

Sample Preparation. All full-length variants of protein L used in this paper were expressed and purified as described in Yi et al. (*12*). Point mutations were made using the QuikChange Site Directed Mutagenesis Kit (Stratagene).

A 42 residue peptide corresponding to the first β-hairpin and helix (pL 1−42) was prepared by Research Genetics. Its sequence is as follows: KVTIKANLIFANGSTQ-TAEWKGTFEKATSEAYAYADTLKKDN. The peptide sequence differs from wild-type in that the glutamate at position 1 was changed to a lysine and the C-terminus was amidated to aid in solubility. Also, position 20 was changed from a phenylalanine to a tryptophan residue to provide an intrinsic fluorophore. The peptide was purified to >90% using HPLC. The 10 mer peptide containing the region surrounding F20W (pL 16−25), QTAEWKGTFE, was also prepared by Research Genetics. The first β-hairpin (pL 2−22), the α-helix (pL 21−45), and the second β-hairpin (pL 43−63) peptides were graciously provided by the Serrano lab (*13*).

IAEDANS Labeling. The proteins were purified using a nickel column followed by a SP sepharose column as described in Yi et al. (*12*). During the purification, the cysteine was kept in the reduced form using 1 mM β-mercaptoethanol in the nickel column and 1 mM TCEP (Molecular Probes) in the SP Sepharose column. For the labeling

† This work was supported by an NIH grant and Young Investigator awards to D.B. from the NSF and the Packard Foundation. S.N. was supported by a Hall-Ammerer-Washington Research Foundation fellowship.

* To whom correspondence should be addressed. Phone: (206) 543-1295. Fax: (206) 685-1792. E-mail: dabaker@u.washington.edu.

[1] Abbreviations: CD, circular dichroism; HD, hydrogen−deuterium; FRET, fluorescence resonance energy transfer; NMR, nuclear magnetic resonance.

10.1021/bi991136g CCC: $18.00
Published on Web 11/09/1999

reaction, the protein solution was adjusted to a final concentration of 200 μM protein, 2.5 M guanidine, 50 mM sodium phosphate, pH 8.0, and 1 mM TCEP (the reaction was done under denaturing conditions to prevent aggregation at higher protein concentrations).

A 2-fold molar excess of 1, 5-IAEDANS was added to the protein solution and the mixture incubated in the dark at 25 °C for 1 h. The labeled protein was purified from the unreacted 1,5-IAEDANS using a Sephadex G25 column equilibrated with 2.5 M guanidine and 50 mM sodium phosphate, pH 7.0. Mass spectrometry analysis indicated that more than 90% of the protein molecules were labeled.

Biophysical Characterization. The dead-time labeling experiments were performed as described in Yi et al. (*10*) and all kinetic and equilibrium experiments were performed as described in Scalley et al. (*9*). For fluorescence energy-transfer experiments, excitation wavelengths were 280 and 336 nm for the tryptophan and the dansyl groups, respectively. To selectively monitor the fluorescence of the dansyl group in the stopped-flow experiments, a 420 nm cutoff filter was used.

FRET Analysis. We used the following scheme to analyze the data from the fluorescence energy-transfer experiments:

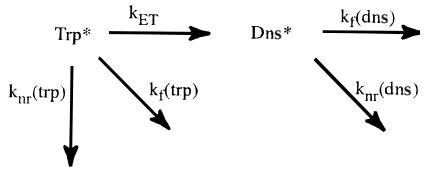

k_{nr} and k_f are nonradiative and radiative decay constants, respectively, for the tryptophan and dansyl excited states (Trp* and Dns*). k_{ET} is the rate of energy transfer from tryptophan to dansyl.

The distance between the tryptophan and dansyl molecules at a given guanidine concentration is reflected in the ratio

$$\frac{k_f(\text{trp})}{k_{ET}} = \frac{Q(\text{trp}) \times Q(\text{dns,int})}{Q(\text{dns})} \quad (1)$$

where the quantum yields, Q(trp), Q(dns), and Q(dns, intrinsic) are defined as

$$Q(\text{trp}) = \frac{k_f(\text{trp})}{k_f(\text{trp}) + k_{ET} + k_{nr}(\text{trp})}$$

$$Q(\text{dns}) = \left(\frac{k_{ET}}{k_f(\text{trp}) + k_{ET} + k_{nr}(\text{trp})}\right) \times \left(\frac{k_f(\text{dns})}{k_f(\text{dns}) + k_{nr}(\text{dns})}\right)$$

$$Q(\text{dns,int}) = \frac{k_f(\text{dns})}{k_f(\text{dns}) + k_{nr}(\text{dns})}$$

The Förster distance for the tryptophan-dansyl pair is ~22 Å, thus, significant changes in the ratio are expected for changes in the tryptophan-dansyl distance in the 10−35 Å range. With the assumption that the extinction coefficient of the dansyl group is independent of guanidine concentrations and the position where it is conjugated to the protein, the quantity on the right in eq 1 is proportional to the following readily measured quantity:

$$\frac{I(\text{trp}) \times I(\text{dns,int})}{I(\text{dns})}$$

where I(trp) is the tryptophan fluorescence intensity, I(dns, int) is the dansyl fluorescence intensity upon excitation at 336 nm, and I(dns) is the dansyl fluorescence intensity upon excitation at 280 nm.

RESULTS

Dead-Time Labeling. Previously, dead-time labeling experiments were performed on protein L to examine whether any amide hydrogens were protected from exchange within the first few milliseconds of folding (*10*). Although large-scale protection was not seen, the results suggested that there may be partial protection within the first β-hairpin and helix region. However, marginally stable structures are difficult to observe using this method since their population may be low. Thus, the experiments were repeated in the presence of a stabilizing agent (sodium sulfate) which has been shown to increase the population of partially folded species in other proteins (*14*).

The proton occupancies measured at 7 of the 19 structural probes in protein L are plotted as a function of labeling pH in Figure 1 (closed circles represent 400 mM sodium sulfate data and open circles represent 800 mM sodium sulfate data). For comparison, calculated curves are included which represent the proton occupancy expected if each amide site displayed random coil exchange behavior (full lines), protection factors of 2 (dashed lines), or protection factors of 5 (dotted lines) throughout the labeling period. In the majority of cases, there is very close agreement between the experimental data and the random coil exchange values, indicating no measurable protection from exchange in the first 3.5 ms of refolding (Figure 1; I4 and E30). However, at the amide sites of A6 and L8, the extent of labeling is less than that expected from the theoretical curve. In both cases, the extent of labeling is less in 800 mM sodium sulfate than in 400 mM sodium sulfate, which is consistent with greater protection from exchange by increased structure formation under more stabilizing conditions. There is also a weaker suggestion of protection at A18, Y32, and A33. While the protection factors are small, the consistency between the results obtained in 0 M, 400 mM, and 800 mM sodium sulfate for the majority of the residues, and the increase in protection factors with increasing sodium sulfate concentrations for a small subset of residues (A6, L8, A18, Y32, and A33) suggests that the weak protection observed derives from structural properties of the denatured state ensemble.

The locations of the five sites at which there may be protection from exchange are indicated in the schematic of protein L structure shown in Figure 2. A6 and L8 both occur within the first strand of the first β-hairpin. A18 occurs in the second strand of this hairpin, directly opposite A6 (the amide hydrogens of each residue hydrogen bond to the carbonyl of the other). Y32 and A33 are located within the α-helical region, which packs up against the section of the first β-hairpin containing the other residues with possible protection, but in the native structure, Y32 and A33 interact more extensively with the second β-hairpin. While the HD exchange protection in the N-terminal half of the protein (the

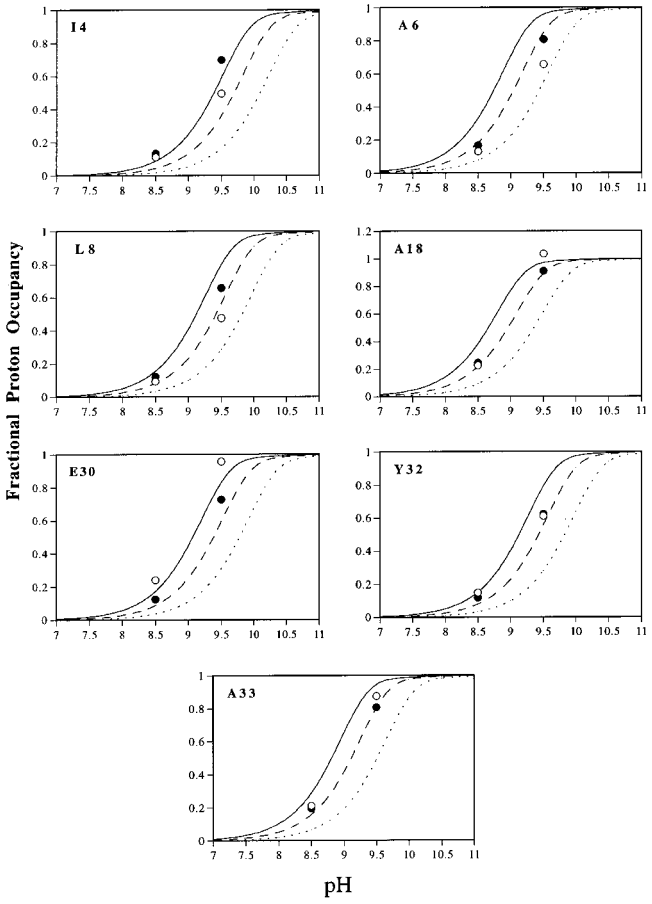

FIGURE 1: Dead-time labeling shows protection factors >1 for residues A6, L8, A18, Y32, and A33. Labeling was performed with 400 mM sodium sulfate (closed circles) and 800 mM sodium sulfate (open circles) with a final guandine concentration of 0.4 M. Lines representing the expected proton occupancy corresponding to a protection factor of 1 (solid line), 2 (dashed lines), and 5 (dotted lines) were calculated using the method in Gladwin et al. (1996).

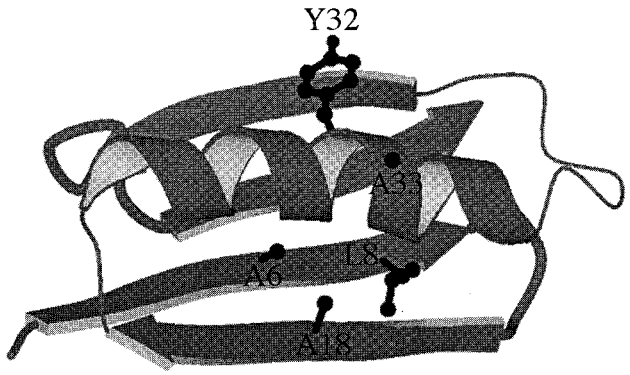

FIGURE 2: Residues in protein L that show protection factors >1. Image was made using the Raster 3D [Bacon and Anderson (1988), Merritt and Murphy (1994)] and Molscript programs [Kraulis (1991)].

first β-hairpin and helix) is suggestive, it must be emphasized that the protection factors are very small even under stabilizing conditions.

F20W Characterization. In previous studies, a fluorophore was introduced into protein L by mutating Y45 to a tryptophan residue, wt(trp) (*9*). Burst phase changes in signal were conspicuously absent for the majority of the methods used to monitor refolding. However, when examining the effect of a fluorescence quenching reagent on the kinetics

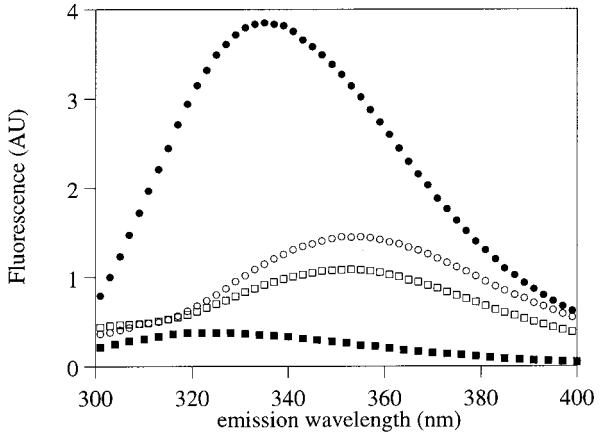

FIGURE 3: Fluorescence emission spectra of wt(trp) and F20W. Wt(trp) and F20W are represented by circles and squares, respectively. Folded conditions (50 mM sodium phosphate, pH 7) are denoted by closed symbols and unfolded conditions (5 M guanidine, 50 mM sodium phosphate, pH 7) by open symbols. Protein concentrations were 10 ± 0.5 μM. The excitation wavelength was 280 nm.

of folding, a dead time gain of signal was observed which would be compatible with a partial collapse involving the first β-hairpin and helix. With this information combined with the dead-time labeling experiments, we decided to place a fluorophore within the first β-hairpin to probe possible structure formation in this region. This was accomplished by mutating F20 to a tryptophan residue (position 45 was reverted to the wild-type tyrosine).

The CD spectra of this mutant (F20W) was similar to that of wt(trp), indicating that the mutation did not cause large structural perturbation (data not shown). The fluorescence emission spectra of F20W is shown in Figure 3. Unlike wt-(trp), F20W experiences a decrease in fluorescence intensity when going from the unfolded (open squares) to the folded state (closed squares) as opposed to wt(trp) whose fluorescence increases upon folding. The tryptophan fluorescence is evidently quenched by nonlocal interactions in the native state.

Equilibrium unfolding of F20W was monitored by both CD and fluorescence. The unfolding transitions obtained by both methods were superimposable (data not shown), suggesting that the loss of tertiary and secondary structure occur simultaneously. The stability of F20W was measured by the linear extrapolation method to be 4.5 kcal mol^{-1}, similar to wt(trp), (4.6 kcal mol^{-1}, see ref *10* for further discussion of the free energy of folding for protein L).

Interestingly, the guanidine melt monitored by fluorescence (Figure 4; open circles) shows that the slope of the unfolded baseline is quite large; the unfolded baseline of wt(trp), in contrast, has a negligible slope (*9*). The slope may be indicative of partial structure being melted out over a broad guanidine concentration or simply due to local sequence effects. To investigate possible local sequence effects, a 10 mer peptide containing the sequence surrounding F20W was obtained and a guanidine melt performed (Figure 4, crosses). The fluorescence of the 10 mer peptide increased with guanidine with a slope similar to that of the F20W unfolded baseline. Thus, local interactions within the 10 residue segment largely account for the observed slope.

The kinetics of F20W refolding were examined using stopped-flow fluorescence. Typically, refolding was initiated

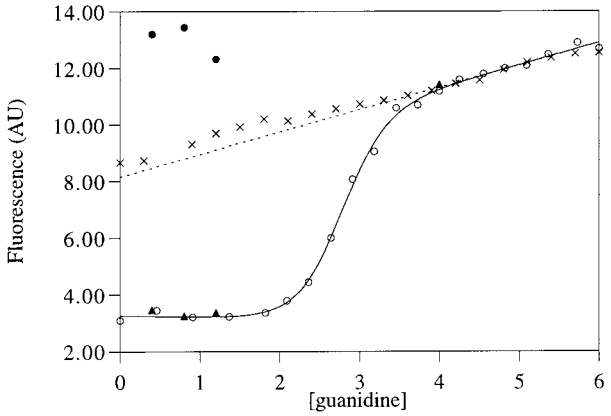

FIGURE 4: Comparison between kinetic and equilibrium data for F20W. The equilibrium denaturation melt monitored by fluorescence (open circles) was fit according to a two state model [solid line (*9*)]. The unfolded baseline was extended to 0 M guanidine (dotted line). The initial values from kinetic experiments (closed circles) were obtained from extrapolation of the fit rate constant through the mixing dead-time (1.7 ms). The final values from kinetic experiments (closed triangles) were used to calculate the appropriate scale factors. Denaturant melt of the 10 mer peptide (crosses) is shown for comparison. An excitation wavelength of 280 nm was used. All experiments were performed in 400 mM sodium sulfate, 50 mM sodium phosphate. Protein concentrations were 10 ± 0.5 μM for kinetic experiments and 5 ± 0.2 μM for equilibrium experiments.

by rapidly diluting the denatured protein into phosphate buffer containing low concentrations of denaturant. Kinetic experiments were performed in the presence of 400 mM sodium sulfate to stabilize possible intermediates. The folding rate of F20W is very similar to that of wt(trp); refolding rates in 0 M guanidine and 400 mM sodium sulfate were 185 s^{-1} for F20W and 210 s^{-1} for wt(trp). This suggests that the rate-limiting step for folding is unchanged by the F20W mutation.

Since the dead-time labeling data suggested that the first β-hairpin and helix may come together early in folding, it was of particular interest to examine the early time points in folding of F20W for the presence of a burst phase or any unexplained signal change within the mixing dead time. All refolding curves were fit well by a single exponential model. To investigate whether the fit rate constant could account for the total signal change, the refolding data was extrapolated back through the mixing dead time (1.7 ms). Since the unfolded signal of F20W in low guanidine concentrations cannot be measured directly, the time zero signals from the kinetic experiments (Figure 4, solid circles) were compared to the extrapolation of the unfolded baseline from equilibrium denaturation experiments [Figure 4, dotted line; the final signals of the refolding curves at [guanidine] = 0.4, 0.8, 1.2, and 4 M (solid triangles) were used to determine the scale factor]. It is interesting to note that the unfolded signals at low guanidine concentrations from kinetic experiments are significantly higher than those expected from equilibrium experiments. This suggests that at low denaturant concentrations the unfolded chain is partially structured in the region of the fluorophore, causing the fluorescence to deviate from what would be seen if local sequence interactions were to dominate, as in the 10 mer peptide.

F20W/Y32A and F20W/Y34A Characterization. To allow the unfolded signal at lower guanidine concentrations to be accessible through equilibrium experiments, we made two

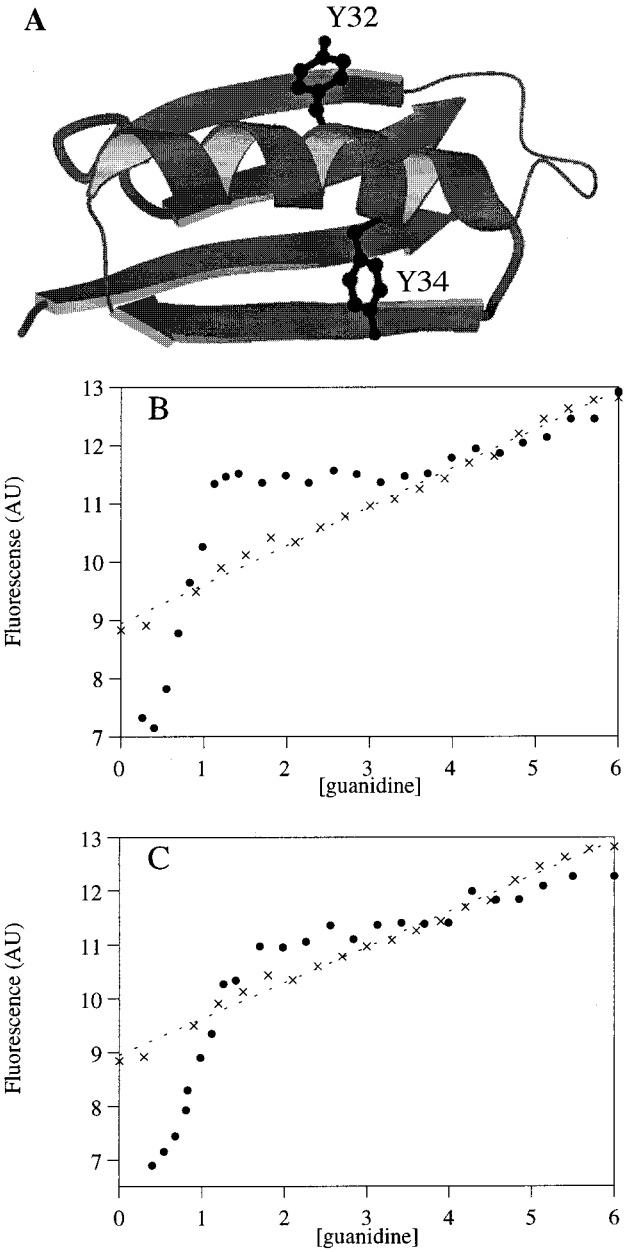

FIGURE 5: Effect of Y32A and Y34A mutations. (A) Schematic of protein L displaying Y32 (upper residue) and Y34 (lower residue). Image was made using the Raster 3D [Bacon and Anderson (1988) and Merritt and Murphy (1994)] and Molscript programs [Kraulis (1991]. (B) Equilibrium denaturation melt for F20W/Y32A (solid circles). (C) Equilibrium denaturation melt for F20W/Y34A (solid circles). Denaturant melt of the 10 mer peptide (crosses) is shown for comparison. An excitation wavelength of 280 nm was used. Protein concentrations were 10 ± 0.5 μM. The differences in the guanidine melts of the two proteins were observed in four independent sets of experiments.

destabilized F20W variants by mutating tyrosine residues in the helix which interact with the first β-hairpin (Y34) and the second β-hairpin (Y32) independently to alanine (Figure 5A). Guanidine melts of both double mutants were performed (Figure 5, panels B and C). In the denaturation curve for F20W/Y32A (Figure 5B, solid circles) there is a plateau in the fluorescence signal between 1.5 and 3.5 M guanidine followed by a gradual increase in fluorescence signal at guanidine concentrations >4 M. The guanidine melt of the 10 mer is shown for comparison (Figure 5, panels B and C, crosses). The 10 mer fluorescence melt is easily aligned with

the sloping region of the F20W/Y32A melt, suggesting that the increase in fluorescence in this region can be explained by local sequence effects. As seen for F20W, the fluorescence signal of F20W/Y32A in low to intermediate guanidine concentrations is higher than expected from the slope of the unfolded baseline at higher guanidine concentrations (>4 M) and the 10 mer peptide data.

Interestingly, the plateau in the intermediate guanidine region is not observed in the F20W/Y34A guanidine melt (Figure 5C, solid circles). Given that the plateau disappears when the interactions between the first β-hairpin and helix are disrupted by the Y34A mutation, it seems likely that it is due to some partial structure in this region of the protein that is stable at intermediate guanidine concentrations.

One possible explanation for the plateau observed at intermediate guanidine concentrations is the occurrence of fluorescence energy transfer between Y34 and W20 which may compensate for the decrease in signal with decreasing guanidine concentration expected given the 10 mer peptide results. Energy transfer between tyrosine and tryptophan residues is possible since the initial experiments were performed using an excitation wavelength of 280 nm where both tryptophan and tyrosine residues are excited. To probe this question, we examined the fluorescence spectra of F20W/Y32A using an excitation wavelength of either 280 or 295 nm at three guanidine concentrations, 2, 3, and 4 M (data not shown). The spectra obtained at a given guanidine concentration were normalized (*15*) and subtracted from one another allowing the peak corresponding to tyrosine fluorescence to be examined. A slight increase in tyrosine fluorescence was observed in 4 M guanidine compared to the spectra taken at lower guanidine concentrations, suggesting that tyrosine−tryptophan energy transfer decreases at higher guanidine concentrations. This result is consistent with structure being present in the region neighboring W20 at intermediate guanidine concentrations. Additionally, the lack of a plateau in the F20W/Y34A guanidine melt might reflect removal of the donor tyrosine residue. However, caution must be taken in such an interpretation of the data since there are multiple tyrosine residues in protein L.

Fluorescence Resonance Energy Transfer. To further assess the extent of ordering early in folding, we turned to fluorescence energy-transfer experiments. Each of three residues in the F20W/Y32A protein L construct was individually mutated to cysteines. The positions correspond to the N-terminus (E1C), the second β-strand (T17C), and the third β-strand (T46C). Figure 6 shows the position of these residues in relation to F20W. The cysteine-containing proteins were purified and dansyl groups were attached to the cysteine residues (see Materials and Methods).

Fluorescence spectra of the labeled cysteine mutants using an excitation wavelength of 280 nm (Figure 7) display a considerable shift in the observed λ_{max} in comparison to that of F20W (Figure 3). To ensure that the observed shift in emission spectra was not due to misfolding of the proteins, CD spectra for each of the cysteine mutants were measured along with F20W and F20W/Y32A (data not shown). The CD spectra of the proteins were virtually superimposable suggesting that all of the proteins were properly folded.

Equilibrium unfolding experiments monitored by fluorescence with an excitation wavelength of 280 nm (to directly excite the tryptophan but not the dansyl groups) showed that both the tryptophan (Figure 7, left, peak at ~360 nm) and the dansyl (Figure 7, left, peak at ~500 nm) fluorescence intensities changed considerably through the unfolding transitions of each of the dansyl derivatized proteins. The changes in dansyl fluorescence during unfolding could be due to changes in (1) the extent of quenching of the donor tryptophan residue, (2) the efficiency of fluorescence energy transfer from the tryptophan to the dansyl group, and/or (3) changes in the extent of quenching of the dansyl group. To assess possibility 3, fluorescence of the dansyl groups was monitored following direct excitation at 336 nm at different guanidine concentrations (Figure 7, right). For all three proteins, there was a roughly 10% increase in dansyl fluorescence when the guanidine concentration was reduced from 2 to 0.5 M.

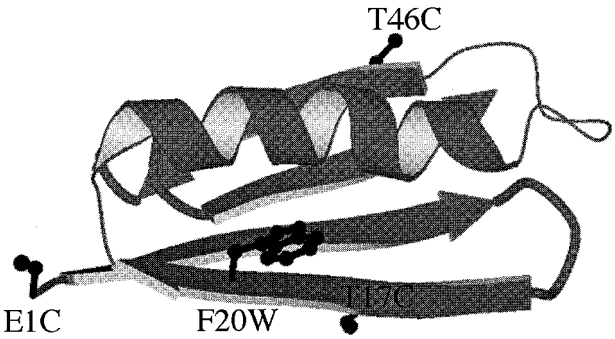

FIGURE 6: Diagram of protein L with the following substitutions: E1C, T17C, F20W, and T46C. The substituted amino acids were integrated into the diagram using the "swap amino acid" feature in Midas (UCSF). The orientations of the substituted amino acids were not computationally optimized. Image was made using the Raster 3D [Bacon and Anderson (1988) and Merritt and Murphy (1994)] and Molscript programs [Kraulis (1991)].

Two different estimates of the efficiency of transfer can be derived from the spectra in Figure 7. The first is the ratio of dansyl fluorescence intensity observed following excitation at 280 nm to that observed following excitation at 336 nm; the denominator corrects for possible differences in the extent of quenching of the fluorescence of the dansyl groups in the different conditions. This ratio (Table 1, left) is highest for the dansyl group at position 17 in the native state and decreases only slightly upon denaturation, consistent with the short sequence separation between the dansyl and the tryptophan. The ratio is considerably higher for the dansyl at position 1 than for the dansyl at position 46 under folded conditions (0.5 M guanidine), consistent with the much smaller distance separation between residue 1 and the tryptophan compared to residue 46 and the tryptophan. A shortcoming of this estimate is the neglect of the dramatic quenching of the tryptophan fluorescence which accompanies folding; this is apparent both in the presence (Figure 7) and absence (Figure 3) of the dansyl labels. A second estimate, which corrects for these differences, is the measure [(tryptophan fluorescence intensity) × (dansyl fluorescence intensity following excitation at 336 nm)/(dansyl fluorescence intensity following excitation at 280 nm)] (see Materials and Methods). This measure (Table 1, right) highlights the difference between the dansyl groups at position 1 and 17; an almost 8-fold change in the former and around a 2-fold change in the latter is observed. There is also a larger change

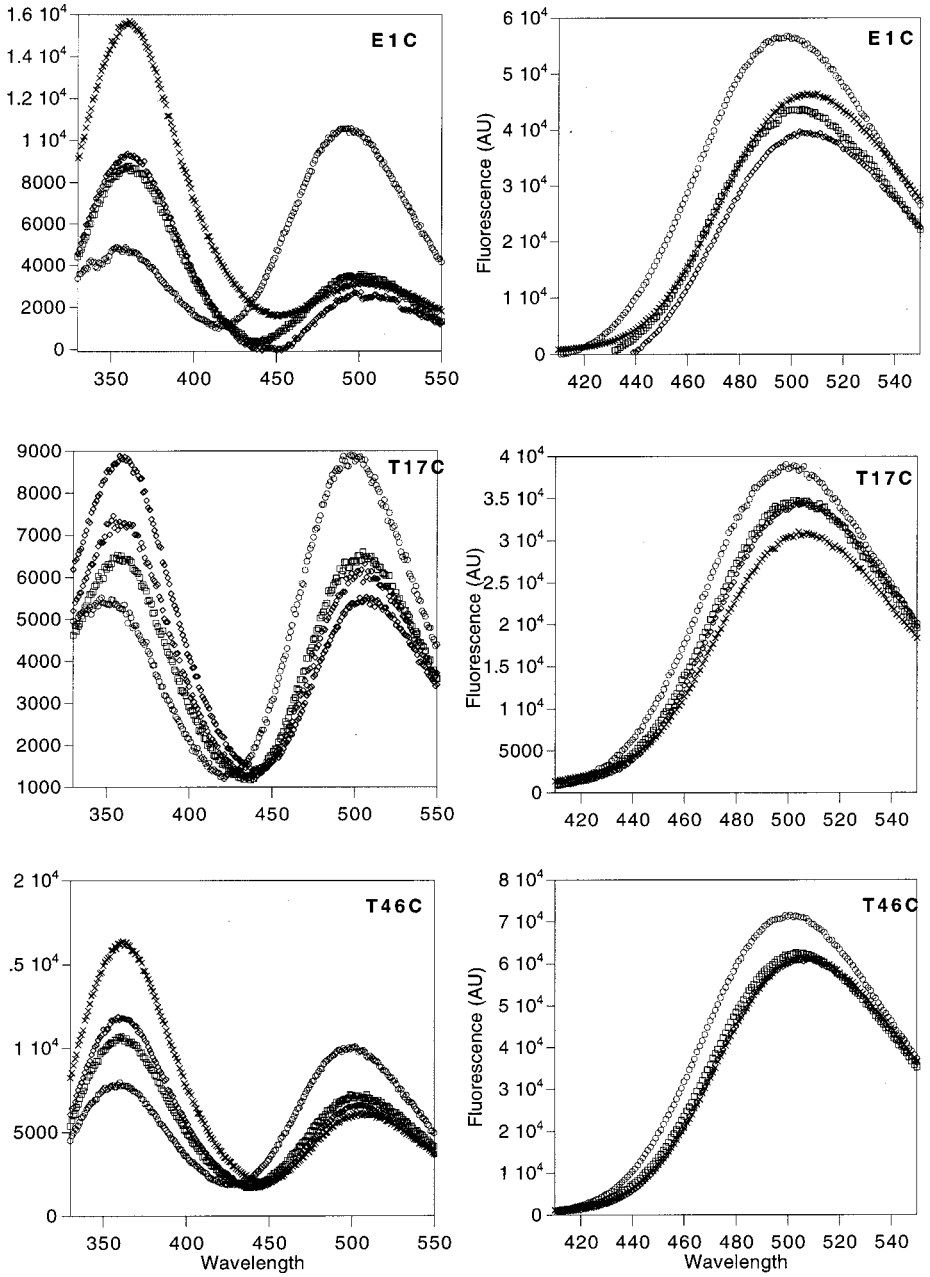

FIGURE 7: Equilibrium fluorescence spectra of dansyl derivatized E1C, T17C, and T46C proteins as a function of guanidine concentration; 0.5 M guanidine (circles), 2 M guanidine (squares), 4 M guanidine(diamond), and 8 M guanidine (crosses). Left panels, excitation at 280 nm. Right panels, excitation at 336 nm. The emission maximum for tryptophan is ~360 nm and that of the dansyl is ~500 nm. Protein concentrations were 7 ± 0.5 μM.

Table 1: Estimates of the Transfer Efficiency between F20W and Attached Dansyl Groups[a]

	I(dns)/I(dns,int)			[I(trp) × I(dns,int)]/I(dns)			
protein	0.5 M gnd	2 M gnd	4 M gnd	0.5 M gnd	2 M gnd	4 M gnd	8 M gnd
E1C	0.40	0.08	0.06	16	68	96	130
T17C	0.20	0.18	0.18	16	24	28	33
T46C	0.14	0.12	0.11	38	61	70	105

[a] I(dns) = dansyl fluorescence intensity following excitation at 280 nm. I(dns,int) = dansyl fluorescence intensity following excitation at 336 nm. I(trp) = tryptophan fluorescence intensity. The quantity on the right is proportional to k_f(trp)/k_{ET} (see Materials and Methods) and is in arbitrary units.

in this quantity in going from 2 to 8 M guanidine for the dansyl at position 1 than for the other two dansyl groups, consistent with some partial ordering of the first hairpin in 2 M guanidine which is abolished in 8 M guanidine.

Stopped-flow fluorescence experiments were used to probe the kinetics of the recovery of dansyl fluorescence during folding. The results for the dansyl at position 1 were dramatic; unlike any of the probes monitored previously, almost all of the large change in dansyl fluorescence upon dilution of the protein from 7.3 M to 0.4 M guanidine occurred within the 1.7 ms deadtime of the stopped-flow device (Figure 8; a 420 nm filter was used to cut off

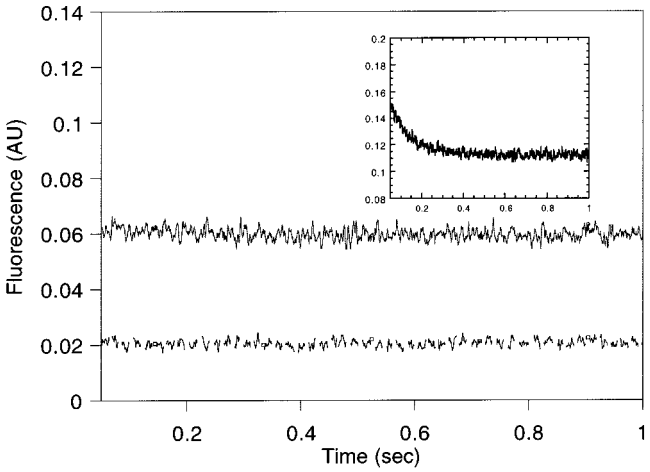

FIGURE 8: The change in dansyl fluorescence during refolding of dansyl derivatized E1C protein occurs on a submillisecond time scale. Denatured protein in 6.2 M guanidine was diluted to 0.4 M guanidine to initiate refolding. Fluorescence energy transfer was monitored by exciting the tryptophan at 280 nm and monitoring the dansyl fluorescence using a 420 nm cut off filter (circles). The signal of the denatured protein diluted in 7.3 M guanidine is shown for comparison (squares). Inset displays the refolding kinetics observed through total fluorescence (tryptophan + dansyl) above 309 nm. Protein concentrations were 10 ± 0.5 μM.

fluorescence directly from the tryptophan). The bulk of the changes in fluorescence intensity of the dansyl groups at the other two positions upon folding were also observed to take place during the deadtime of the instrument (data not shown). The change in intrinsic fluorescence of the dansyl group following the excitation at 336 nm also occurred within the instrument dead time (data not shown). To determine the folding rate under these conditions, the total change in fluorescence intensity above 309 nm was also monitored for the protein containing dansyl at position 1 (Figure 8, inset); the refolding of the protein was readily observed, and the dansyl modification was found to slow the refolding rate roughly 2-fold. Although orientational and environmental contributions to fluorescence and fluorescence energy-transfer efficiency that are difficult to quantify complicate the quantitative interpretation of these data, the results clearly demonstrate that conformational changes involving the dansyl and tryptophan residues occur very early (<1 ms) in protein L folding.

Peptide Studies. Since it appeared that the first region of the protein may form partial structure in the denatured state, we examined a 42 mer peptide of protein L comprised of the first β-hairpin and α-helix (residues 1−42, see Materials and Methods for sequence). The peptide was found to be soluble to ∼100 μM in 50 mM sodium phosphate buffer, pH 6, and the CD spectra were identical for varying concentrations of peptide, suggesting that aggregation did not occur under these conditions. CD spectra of the 42 mer were taken in both 0 and 5 M guanidine (Figure 9A, solid circles and open circles, respectively). The difference between the two spectra is shown in Figure 9B; the difference spectrum resembles that of an α-helix with a minimum close to 222 nm, indicating population of helical structure. The minimum at 222 nm was used to calculate the percent helicity present in 0 M guanidine (*16*); the percent helicity was found to be ∼7%. Were the helix in the native structure fully formed in the peptide, the percent helicity of the peptide

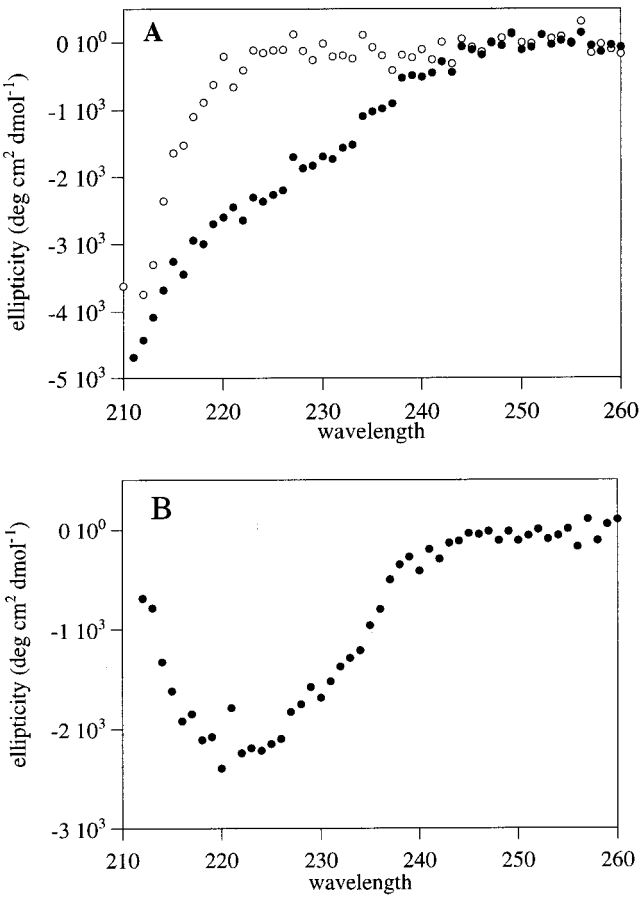

FIGURE 9: Effect of denaturant on 42 mer CD spectra. (A) The CD spectra of the 42 mer peptide was measured in 50 mM sodium phosphate, pH 7 (closed circles) and 5 M guanidine and 50 mM sodium phosphate, pH7 (open circles); (B) The difference spectra. Protein concentrations for CD spectra in panel A were 18 ± 0.5 μM.

would be 35%. These numbers suggest that 20% of the helix that is formed in intact protein L is also formed in the isolated peptide. This percentage is probably an underestimate since the percent helix in full-length protein L was calculated to be 12% using the Gans et al. (*16*) method compared to 24% obtained from the solution structure. The CD signal of the 42 mer was found to have a linear dependence on guanidine concentration (data not shown). Therefore, the loss of secondary structure in the 42 mer does not appear to be highly cooperative.

In previous studies conducted by Ramirez-Alvarado et al. (*13*), three peptides corresponding to the first β-hairpin (pL1), the α-helix (pL2), and the second β-hairpin (pL3) were studied in detail. Using CD and NMR, it was found that both pL1 and pL3 contained small populations of locally folded species with native and non-native interactions. pL2 was calculated to have a helical content of ∼4% although aggregation complicated its analysis.

Comparison of the amount of helical structure in the 42 mer peptide and pL2 (which contains only helical residues) provides a means to investigate interactions between the first β-hairpin and the helix that may favor helix formation. Experiments were performed at pH2 to minimize aggregation of pL2. The spectrum of the 42 mer has a greater negative ellipticity between 215 and 235 nm than that of pL2 (Figure 10). PL2 contains a higher percentage of native helical

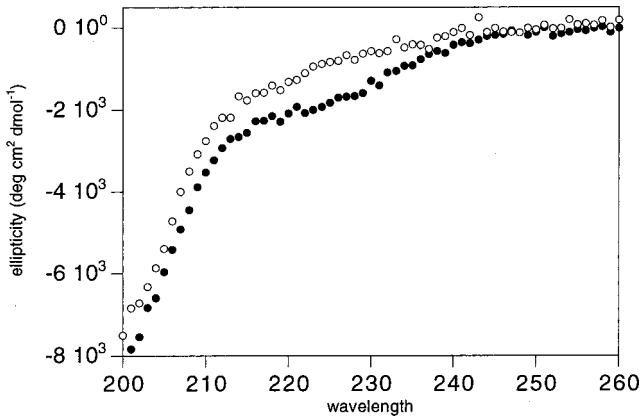

FIGURE 10: CD spectra of helix peptide, pL2, (open circles) and 42 mer peptide (closed circles). Buffer conditions were 50 mM sodium phosphate, pH 2. Concentrations of pL2 and the 42 mer were 26 and 14 μM, respectively. The pL2 sample contained 1.3% HFIP; this percentage was shown to have no effect on the CD spectra of pL2.

residues than does the 42 mer and since Figure 10 shows molar residue ellipticities, if only native helix is formed in both cases the population of this helix must be significantly higher in the longer peptide.

Previously, peptides of varying lengths for both CI2 (*17*) and Barnase (*18*) were probed for the presence of nativelike interactions. Interestingly, even the longest peptide fragment of CI2, residues 7−64, did not populate nativelike structures. For Barnase, however, it was seen that a fragment lacking the first two α-helixes, B23−110, was capable of folding to a nativelike state. Studies on peptide fragments of protein L appear to be more similar to those described for CI2, since only a small amount of structure was observed. This is not surprising since CI2 and protein L are small compared to Barnase; the B23−110 fragment of Barnase is larger than both native CI2 and protein L.

Complementation studies were performed with the 42 mer peptide and the peptide containing the second β-hairpin, pL3, to see whether additional structure could be formed. Previous studies on protein G, a structurally similar protein, showed peptide fragments were able to complement one another to yield native structure (*19*). The sum of the individual spectra compared to the spectrum of both peptides together is shown in Figure 11A. For comparison, Figure 11B displays the resulting difference spectrum along with the spectrum of full-length protein L. The difference spectrum is similar in shape to that of full-length protein L; however, the minimum of the difference spectrum, 220 nm, is shifted to the far-UV compared to full-length protein L. Thus, the structure being formed by the complementation experiments may not be entirely nativelike. This possiblity is also supported by fluorescence studies that showed no change in fluorescence emission when the two peptides were combined; a decrease in fluorescence would be expected if nativelike structure was formed. The two peptides thus appear to form a structure with more α-helix than the isolated 42 mer peptide but less β-sheet and a less well-ordered core than intact protein L.

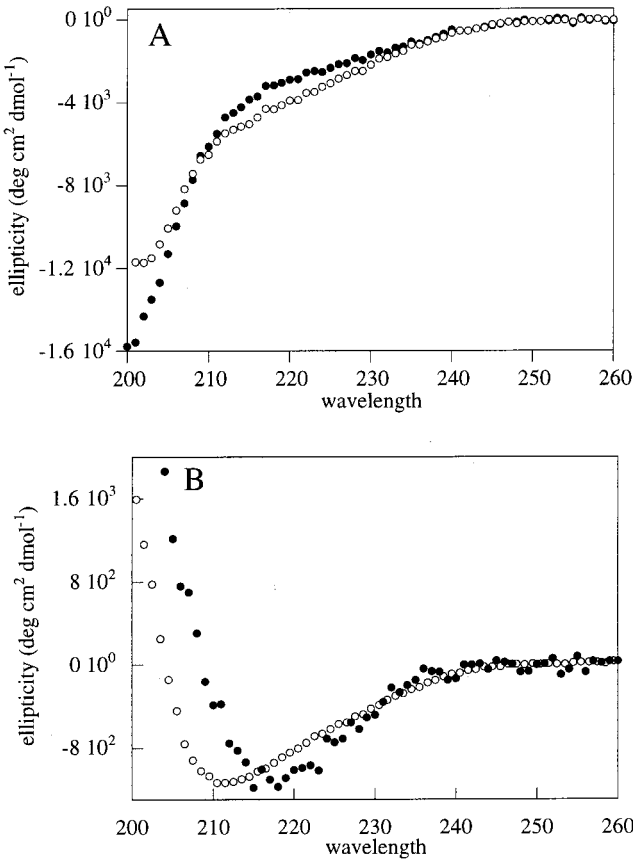

FIGURE 11: Peptide complementation experiments. (A) Sum of the individual spectra of 42 mer and pL3 (closed circles) and the spectra of 42 mer peptide combined with pL3 (open circles). (B) Difference spectra between the two spectra described in panel A (closed circles) and the spectra of full-length protein L (open circles). The full-length protein L spectra was multiplied by 0.158 to aid in comparison. Buffer conditions were 50 mM sodium phosphate, pH 6. Concentrations of pL3, 42 mer, and both in combination were 26 ± 2 μM.

DISCUSSION

Dead-time labeling experiments performed in the presence of sodium sulfate show that a small amount of protection from HD exchange occurs for residues within the first β-hairpin and the helix: A6, L8, A18, Y32 and A33. Placement of a fluorophore within the first β-hairpin (F20W) facilitated examination of this area. It became evident through comparisons of kinetic and equilibrium data that in low to intermediate denaturant concentrations the residues near the fluorophore are structured so as to alter the fluorescence of the unfolded protein. To access the unfolded signal of the protein at low guanidine concentrations more readily with equilibrium experiments, two destabilized F20W mutants were made. Guanidine denaturation studies of F20W/Y32A, a mutant where the interaction between the second β-hairpin and helix are destabilized, show that the signal from the unfolded protein at low to intermediate guanidine concentrations deviates from that of the expected value given local sequence effects alone. Interestingly, this effect is missing in the F20W/Y34A mutant where interactions between the first β-hairpin and the helix are disrupted. Fluorescence energy-transfer experiments also suggest partial ordering in this region and that the ordering occurs on a submillisecond time scale upon a change in solvent conditions.

Peptide studies on the 42 mer containing the first β-hairpin and the α-helix indicate this region of the protein is able to independently populate stable, helical structures. To determine whether the presence of the first β-hairpin promotes population of helical structures the amount of helix in the

42 mer was compared to that in the isolated helix peptide, pL2. The percent helix was found to be higher in the 42 mer than in pL2, indicating the presence of helix stabilizing interactions between the first β-hairpin and α-helix. Furthermore, complementation studies with the 42 mer peptide and the second β-hairpin led to the formation of additional structure (although the structure may not be completely nativelike). These data suggest that interactions within the β-hairpin and α-helix lead to partial folding of this region independent of the entire protein.

Recent solution X-ray scattering studies showed that protein L does not undergo a rapid collapse in early refolding in 1.4 M guanidine (*20*); the radius of gyration of the unfolded protein early in refolding is indistinguishable from that of the denatured protein. Thus, the local ordering around the tryptophan residue observed here occurs in conformations that are still quite extended, perhaps because the last two strands remain fairly disordered. Such a picture is consistent with preliminary NMR characterization of the denatured protein in 2 M guanidine (Q. Y. and D. B., unpublished results).

A puzzling feature of the folding of protein L is that the symmetry of the protein (evident in Figure 2) is completely broken in the folding transition state; mutations in the first β-turn slow the folding rate and have little effect on the unfolding rate, while mutations in the second β-turn increase the unfolding rate but have virtually no effect on the folding rate. The results in this paper suggest that this asymmetry is already present in the denatured state ensemble under refolding conditions and is established very early after initiation of refolding.

ACKNOWLEDGMENT

We would like to thank Marina Ramirez-Alvarado and the Serrano Lab for supplying the protein L peptide fragments. We would also like to thank an anonymous reviewer for suggesting the scheme described in Materials and Methods for interpreting the FRET data and members of the Baker Lab for insightful comments on the manuscript.

REFERENCES

1. Huang, G. S., and Oas, T. G. (1993) *Biochemistry 32*, 11270−11278.
2. Jackson, S. E., elMasry, N., and Fersht, A. R. (1995) *Biochemistry 34*, 3884−3892.
3. Khorasanizadeh, S., Peters, I. D., and Roder, H. (1996) *Nat. Struct. Biol. 3*, 193−205.
4. Kragelund, B. B., Robinson, C. V., Knudsen, J., Dobson, C. M., and Poulsen, F. M. (1995) *Biochemistry 34*, 7217−7224.
5. Milla, M. E., and Sauer R. T. (1994) *Biochemistry 33*, 1125−1133.
6. Sosnick, T. R., Mayne, L, and Englander, S. W. (1996) *Proteins: Struct., Funct., Genet. 24*, 413−426.
7. Villegas, V., Azuaga, A., Catasus, Ll., Reverter, D., Mateo, P. L., Aviles, F. X., and Serrano, L. (1995) *Biochemistry 34*, 15105−15110.
8. Zitzewitz, J. A., Bilsel, O., Luo, J., Jones, B. E., and Matthew, C. R. (1995) *Biochemistry 34*, 12812−12819.
9. Scalley, M. L., Yi, Q., Gu, H., McCormack, A., Yates, J. R., and Baker, D. (1997) *Biochemistry 36*, 3373−3382.
10. Yi, Q., Scalley, M. L., Simons, K. T., Gladwin, S. T., and Baker, D. (1997) *Folding Des. 2*, 271−280.
11. Gu, H., Kim, D., and Baker, D. (1997) *J. Mol. Biol. 274*, 588−596.
12. Yi, Q. a. B., D. (1996) *Protein Sci. 5*, 1060−1066.
13. Ramirez-Alvarado, M., Serrano, L., and Blanco, F. J. (1997) *Protein Sci. 6*, 162−174.
14. Sauder, J. M. a. R., H. (1998) *Folding Des. 3*, 293−301.
15. Murthy, U. S., Podder S. K., Adiga, P. R. (1976) *Biochim. Biophys. Acta 434*, 69−81.
16. Gans, P. J., Lyu, P. C., Manning, M. C., Woody, R. W., and Kallenbach, N. R. (1991) *Biopolymers 31*, 1605−1614.
17. Ladurner, A. G., Itzhaki, L. S., de Prat-Gay, G., and Fersht, A. R. (1997) *J. Mol. Biol. 273*, 317−329.
18. Niera, J. L. a. F., A. R. (1999) *J. Mol. Biol. 287*, 421−432.
19. Honda, S., Kabayashi, N., Munekata, E., and Uedaira, H. (1999) *Biochemistry 38*, 1203−1213.
20. Plaxco, K. W., Millett, I. S., Segal, D. J., Doniach, S., and Baker, D. (1999) *Struct. Biol. 6*, 554−557.

BI991136G